IECEC-97

PROCEEDINGS OF THE THIRTY SECOND

INTERSOCIETY ENERGY CONVERSION ENGINEERING CONFERENCE

VOLUME 4

Post Deadline Papers
Index

July 27 - August 1, 1997
Honolulu, Hawaii

American Institute of Chemical Engineers
345 East 47th Street, New York, NY 10017

IECEC-97

PROCEEDINGS OF THE THIRTY-SECOND

INTERSOCIETY ENERGY CONVERSION ENGINEERING CONFERENCE

VOLUME 4

Post Deadline Papers
Author Index

July 27 - August 1, 1997
Honolulu, Hawaii

American Institute of Chemical Engineers
345 East 47th Street, New York, NY 10017



Table of Contents

Volume 4
Post Deadline Papers
and Author Index

AEROSPACE POWER SYSTEMS AND TECHNOLOGIES

SPACE SOLAR, NUCLEAR AND OTHER ENERGY CONVERSION SYSTEMS

AEROSPACE POWER ELECTRONICS AND ANALYSIS

SPACECRAFT, AIRCRAFT AND INTERNATIONAL SYSTEMS

SPACE STATION POWER

ELECTRO-CHEMICAL TECHNOLOGIES

BATTERIES

CONVERSION TECHNOLOGIES

COMBUSTION SYSTEMS

THERMIONICS AND THERMOELECTRICS

ADVANCED THERMAL AND RELATED SYSTEMS

INNOVATIVE CONCEPTS

THERMAL MANAGEMENT

HEAT PIPES AND HEAT TRANSFER

ENERGY SYSTEMS

BUILDING AND THERMAL ENERGY SYSTEMS

POWER AND ENERGY STORAGE SYSTEMS

RENEWABLE ENERGY RESOURCES

BIOMASS

PHOTOVOLTAICS AND HYDROGEN

ENVIRONMENTAL IMPACT

CARBON DIOXIDE AND OTHER ENVIRONMENTAL ISSUES

POLICY IMPACTS ON ENERGY

CASSINI RTG ACCEPTANCE TEST RESULTS AND RTG PERFORMANCE ON GALILEO AND ULYSSES

C. Edward Kelly
Lockheed Martin Corporation
P.O. Box 8555, 29B41-KB
Philadelphia, Pennsylvania 19101

Paul M. Klee
Lockheed Martin Corporation
P.O. Box 8555, 29B41-KB
Philadelphia, Pennsylvania 19101

ABSTRACT

Flight acceptance testing has been completed for the RTGs to be used on the Cassini spacecraft which is scheduled for an October 6, 1997 launch to Saturn. The acceptance test program includes vibration tests, magnetic field measurements, mass properties (weight and c.g.) and thermal vacuum test. This paper presents the thermal vacuum test results. Three RTGs are to be used, F-2, F-6, and F-7. F-5 is the back-up RTG, as it was for the Galileo and Ulysses missions launched in 1989 and 1990, respectively. RTG performance measured during the thermal vacuum tests carried out at the Mound Laboratory facility met all specification requirements. Beginning of mission (BOM) and end of mission (EOM) power predictions have been made based on these tests results. BOM power is predicted to be 888 watts compared to the minimum requirement of 826 watts. Degradation models predict the EOM power after 16 years is to be 640 watts compared to a minimum requirement of 596 watts. Results of small scale module tests are also shown. The modules contain couples from the qualification and flight production runs. The tests have exceeded 28,000 hours (3.2 years) and are continuing to provide increased confidence in the predicted long term performance of the Cassini RTGs. All test results indicate that the power requirements of the Cassini spacecraft will be met. BOM and EOM power margins of over five percent are predicted. Power output from telemetry for the two Galileo RTGs are shown from the 1989 launch to the recent Jupiter encounter. Comparisons of predicted, measured and required performance are shown. Telemetry data are also shown for the RTG on the Ulysses spacecraft which completed its planned mission in 1995 and is now in the extended mission.

INTRODUCTION

The GPHS RTGs which were developed for the Galileo and Ulysses missions have been previously described (Hemler, 1992). The units provide a nominal 300 W(e) with a fuel loading of 4,400 W(th), utilize silicon germanium thermoelectric elements, a molybdenum multi-foil thermal insulation system, and an aluminum outer shell. They weigh 55.3 kg, are 1 meter long and have a fin envelope of approximately 0.4 meters. The RTGs (F-1, F-4) on Galileo have continued to exceed power requirements since the October 1989 launch. Similarly, the Ulysses RTG (F-3) has met all mission power requirements since the October 1990 launch. Two new GPHS type RTGs (F-6 and F-7) have been built under the Cassini program. The third unit, F-2, was built during the Galileo program but never fueled. The backup unit F-5 was built, fueled and flight qualified under the Galileo program. All of the units have undergone the Cassini flight acceptance program and are fully qualified for the scheduled October 6, 1997 launch to Saturn. Three RTGs will provide the power for the Cassini spacecraft and are required to provide a minimum of 826 W(e) at the beginning of mission (BOM) and 596 W(e) after sixteen (16) years (EOM). If the backup unit is used the BOM and EOM requirements are 799 W(e) and 579 W(e), respectively. Small scale 18 couple module tests were used to demonstrate the initial and long term electrical performance of the thermopile as discussed in the next section.

CASSINI MODULE TEST PROGRAM

The Cassini module test program consisted of three 18 couple modules. The purpose of the testing was to demonstrate that the unicouples made for the Cassini RTGs had the same performance characteristics as those used in the Galileo and Ulysses RTGs. Two modules were operated at higher than normal temperature to obtain accelerated life data and the third was operated at normal temperature. Tests results are shown in Figures 1 through 6. Figures 1 and 2 show the power output and internal resistance trends for the Cassini modules 18-10 and 18-11 operated at the accelerated temperature of 1408 K. Also shown for comparison are the trends for modules from the Galileo/Ulysses program. Similar plots are shown in Figures 3 and 4 for module 18-12 which was operated at the normal hot shoe temperature of 1308 K. Thermopile electrical characteristics were found to be in good agreement with previous units. Figures 5 and 6 provide the isolation resistance trends between the thermoelectric circuit and foil insulation system for modules operated at 1408 K and 1308 K, respectively. These trends demonstrate that the silicon nitride coating applied to the thermoelements to suppress sublimation and insure long life has been successfully reproduced in the Cassini unicouples. The comparative performance of the

modules provides a high degree of confidence that the Cassini unicouples will provide the same electrical performance as the Galileo and Ulysses unicouples.

CASSINI FULL SCALE CONVERTER TESTS

RTG F-5

RTG F-5, which serves as the backup RTG for the Cassini mission, completed acceptance testing in October 1995. This unit was fueled at the end of 1984 and also served as the backup RTG for Galileo and Ulysses. Thermal vacuum power measured following vibration testing is shown in Table 1. Power output was 259 W(e) with a fuel loading of 4091 W(th). This is the power at the RTG connector pins. Three watts were added to the measured power to account for the gas venting differences between the test configuration and a flight PRD (pressure relief device). Based on these test results the BOM (beginning of mission) power output is projected to be 251 We with a fuel load of 4029 W(th). EOM (end of mission) power calculated from degradation models is predicted to be 183 W(e). The specification requirements are 249 W(e) BOM and 182 W(e) EOM This unit had the longest storage time ever experienced by an RTG. Internal resistance trends during storage clearly show the reversible nature of the dopant precipitation process. Storage condition is short circuit with hot and cold junction temperatures of 1003 K and 493 K. Prior to launch the hot junction temperature is raised to over 1173 K during an argon to xenon gas exchange process. During this process, previously precipitated dopant redissolves in certain temperature regions of the thermoelements. This results in a decrease in internal resistance when the unit is returned to storage conditions as shown in Figure 7. The net result is that RTGs can be stored in the fueled state and exhibit very little power degradation other than that associated with fuel decay. In fact, F-5 with 10 years of storage between thermal vacuum tests degraded by only two percent when normalized to a constant fuel loading.

TABLE 1. MEASURED AND PROJECTED POWER OUTPUT

	Measured Watts	BOM Fuel	Projected Watts	
UNIT			BOM	EOM
F-2	301.2	4378	296	213
F-6	299.2	4407	294	212
F-7	302.6	4397	298	215
F-5	261	4029	251	183
F-2, F-6, F-7		13182	888	640
F-2, F-5, F-6		12814	841	608

RTG F-2

F-2 was tested as an ETG in 1983 then put in storage at Mound Laboratory. RTG F-2 was fueled at Mound in February 1996 and completed flight acceptance testing in September 1996. At the end of the thermal vacuum test the power output at the connector pins was 301.2 W(e) with a fuel loading of 4416 W(th). Two watts were added to the measured power to account for venting differences between the test configuration and a flight PRD (pressure relief device). Table 1 summarizes measured and predicted performance. A BOM power output of 296 W(e) is predicted with a fuel loading of 4378 W(th). The specification requirement is 274 W(e). The large margin is due to the fact that the BOM fuel loading is higher than originally planned. A BOM fuel loading as low as 4,258 W(th) had been anticipated based on fuel enrichment and packing density estimates available earlier in the program. EOM power is predicted to be 213 W(e) with a specification requirement of 198 W(e).

RTG F-6

F-6 was fueled at Mound Laboratory in November 1996. Power output at the end of the thermal vacuum test was 299.2 W(e) at the RTG pins including a 2 W(e) GMV power correction. The fuel loading at that time was 4430 W(th). Table 1 summarizes measured and predicted performance. A BOM power of 294 W(e) is predicted with a fuel loading of 4407 W(th). The specification requirement is 276 W(e). The BOM power prediction has been decreased by 2 W(e) as an allowance for power loss due to air infusion. Gas tap data analysis showed higher than normal nitrogen levels. There will be some oxidation of moly foil which will increase heat losses slightly. EOM power is predicted to be 212 W(e) with a requirement of 199 W(e).

RTG F-7

F-7 was fueled in September 1996. Thermal inventory at the time of the thermal vacuum test in November 1996 was 4428 W(th). Power output at the end of thermal vacuum testing was 302.6 W(e) at the RTG pins including a 2 W(e) GMV power correction. Measured and predicted performance are given in Table 1. 298 W(e) is predicted for B.O.M compared to the requirement of 276 W(e). EOM power is predicted to be 215 W(e).

The total Cassini spacecraft BOM power specification requirement is 799 We using RTGs F-2, F-5, and F-6. Predicted power based on thermal vacuum measurements is 841 W(e) for a 5 percent margin. Similarly, for RTGs F-2, F-6, and F-7 the specification is 826 W(e) with a predicted power of 888 We for a 7 percent margin. EOM specification and projections are 579 We and 608 We, respectively, for RTGs F-2, 5, and 6 and 596 We and 640 We, respectively, for RTGs F-2, 6 and 7. EOM margins are calculated to be 5 and 7 percent.

GALILEO RTG PERFORMANCE

The Galileo spacecraft was launched in October 1989 on a six year journey to explore Jupiter and its surrounding moons. It arrived on December 7, 1995 after a circuitous route that involved Earth flybys in 1990 and 1992. It is interesting to note that the smaller Voyager spacecraft on a direct trajectory flew by Jupiter eighteen months after launch. Telemetry data have been provided by JPL during the Galileo mission and the power profile is shown in Figure 8 up to September 1996. The power is calculated at the spacecraft bus by multiplying the measured current from each RTG by the constant bus voltage. The accuracy of the measured current is estimated to be ± 1.2 % which corresponds to ± 3 We for the power from each RTG. Initial power was reported as 577 We which was 9 We above the specification requirement. RTG power output has continued to exceed spacecraft required power throughout the mission.

ULYSSES RTG PERFORMANCE

The Ulysses spacecraft was launched in October 1990 with a single RTG, F-3. Its trajectory led it to the planet Jupiter, where in February 1992, it received a gravitational assist that sent it out of the plane of the Earth's orbit and eventually over the poles of the sun. It passed over the south pole in October 1994 and the north pole in 1995. Ulysses completed its original 4.7 year mission in August 1995 and is now in an extended mission of a second polar orbit. The power estimates for F-3 are shown in Figure 9. Unlike Galileo there is no direct measurement of RTG power output. RTG power output is estimated from an algorithm which considers (1) the main bus current, (2) an internal power dump current, and (3) nominal power consumption values for ten spacecraft components if they are operating at the time. Initial telemetry power was reported to be 289 W(e) at the RTG connector which exceeded the specification requirement of 277 W(e). (The prelaunch prediction of BOM power was in the range 282 to 287 W(e). The RTG continued to meet all spacecraft power requirements throughout the 42,000 hour (4.8 year) mission. The EOM power requirement was 245 W(e). JPL has reported that during the periods leading up to an following perihelion in March 1995, there were several spacecraft power reconfigurations in response to the large changes in solar heating as the spacecraft-Sun distance decreased and then increased. Since the algorithm used to estimate power is configuration dependent, these reconfigurations have clearly introduced artifacts into the data set.

CONCLUSIONS

Test results indicate that the BOM and EOM power requirements for the Cassini spacecraft will be met by three RTGs with a power margin of five percent. Telemetry data from the Galileo and Ulysses spacecraft show that all mission power requirements have been met.

ACKNOWLEDGMENTS

The authors acknowledge with thanks the many contributions made by the staffs of the Lockheed Martin Corporation, EG&G Mound Applied Technologies, Savannah River Plant and Laboratory, Los Alamos National Laboratory, Oak Ridge National Laboratory, Sandia National Laboratories, Ames Laboratory, Orbital Sciences, NUS Corporation, the Applied Physics Laboratory, Westinghouse Hanford Company, and Battelle Columbus Laboratories in the design, analysis, fabrication and testing of the GPHS-RTGs, and their components.

Acknowledgments with thanks is also given to R. Campbell of JPL who provided the flight data for Galileo and Ulysses and also valuable consultation regarding interpretation of the data.

REFERENCES

Hemler, R. J. et al, 1992, "Flight Performance of Galileo and Ulysses RTGs," Proceeding of the Ninth Symposium on Space Nuclear Power Systems, Albuquerque, New Mexico, 12-16 January 1992, American Institute of Physics Conference Proceedings 246, 1:171-176.

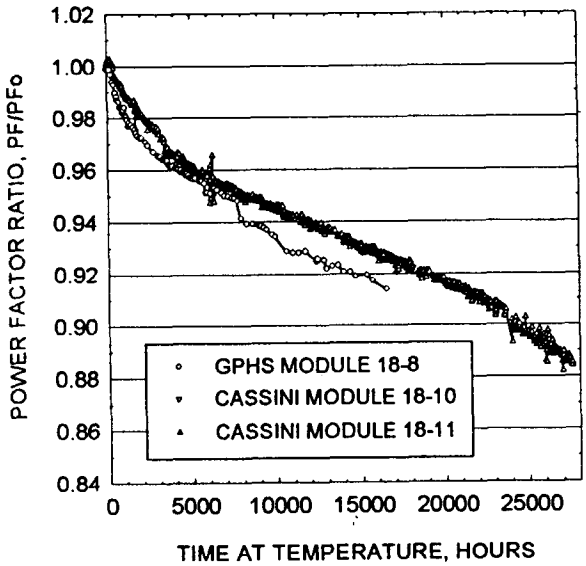

FIGURE 1. 18 COUPLE MODULE POWER FACTOR VERSUS TIME (1408 K OPERATION)

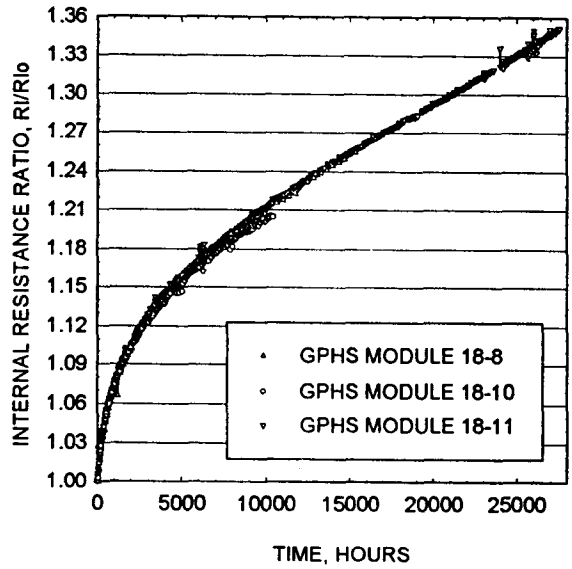

FIGURE 2. 18 COUPLE MODULE INTERNAL RESISTANCE RATIO VERSUS TIME (1408K OPERATION)

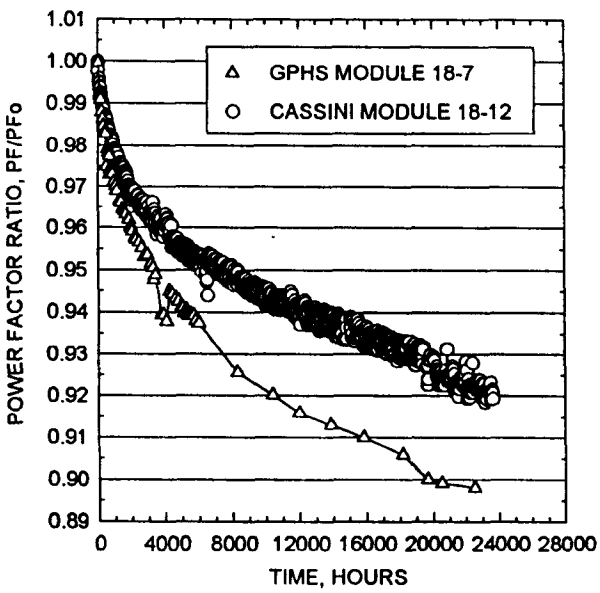

FIGURE 3. 18 COUPLE MODULE POWER FACTOR RATIO VERSUS TIME (1308 K OPERATION)

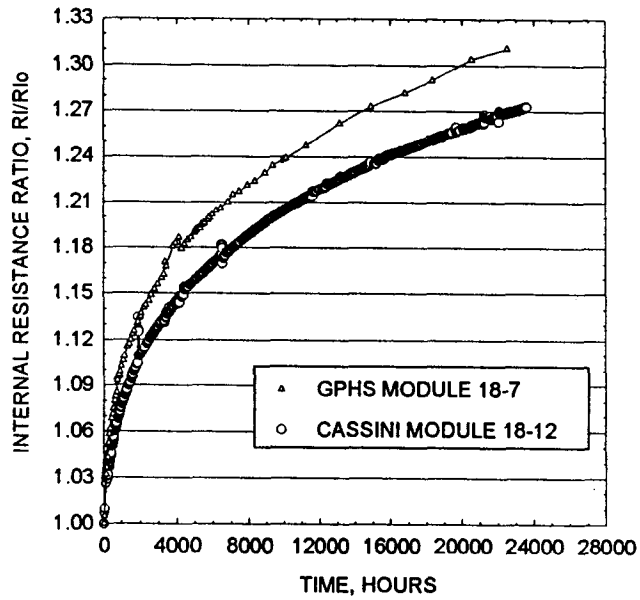

FIGURE 4. 18 COUPLE MODULE INTERNAL RESISTANCE RATIO VERSUS TIME (1308 K OPERATION)

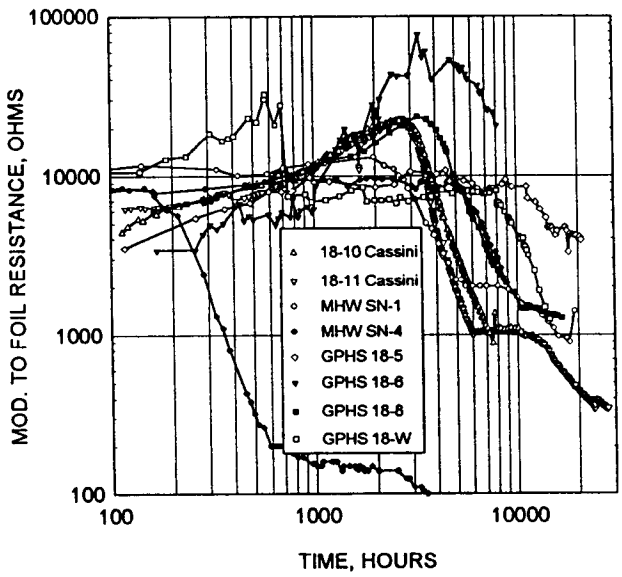

FIGURE 5. ISOLATION RESISTANCE VERSUS TIME (1408 K OPERATION)

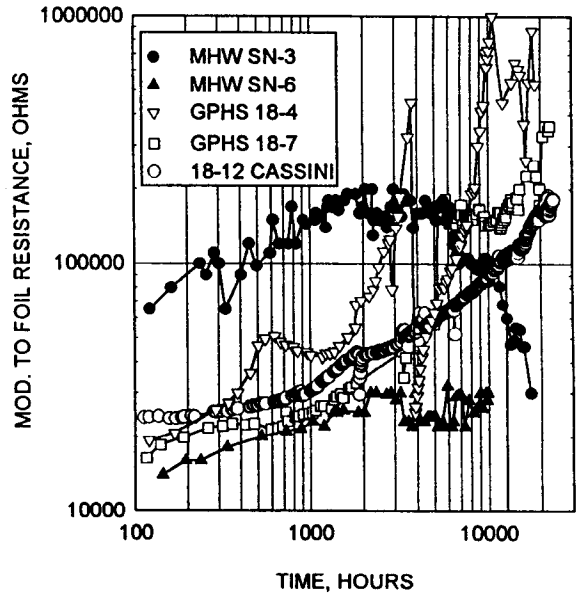

FIGURE 6. ISOLATION RESISTANCE VERSUS TIME (1308 K OPERATIONS)

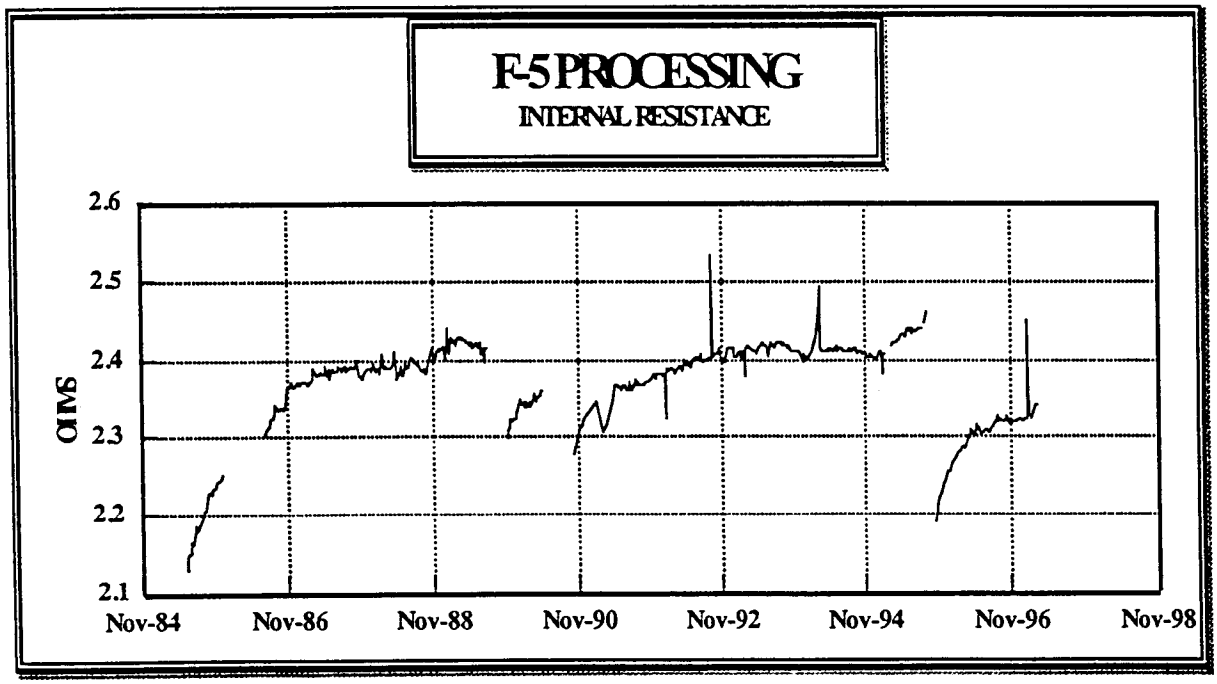

FIGURE 7. F-5 INTERNAL RESISTANCE TRENDS

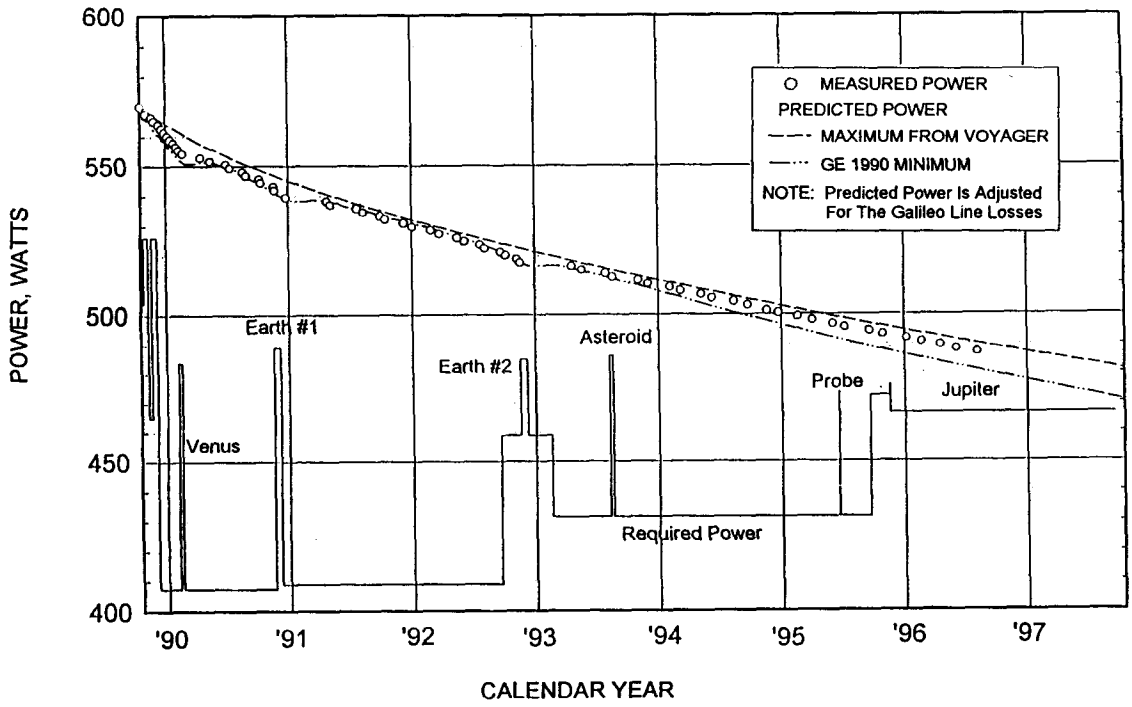

FIGURE 8. GALILEO SPACECRAFT RTG POWER VERSUS TIME
(LAUNCH OCTOBER 18, 1989)

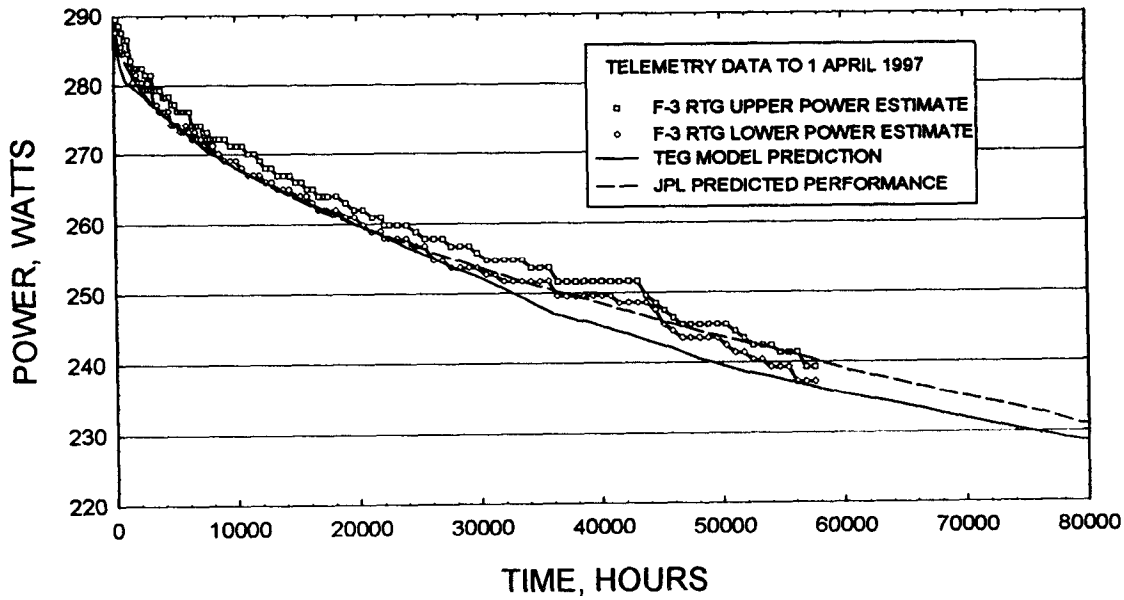

FIGURE 9. ULYSSES SPACECRAFT RTG POWER
(LAUNCH OCTOBER 6,1990)

ANALYSIS OF DC/DC CONVERTERS WITH RESONANT FILTERS

Rene J Thibodeaux
U. S. Air Force/Wright Laboratory
WL/POOC
1950 Fifth Street
Wright-Patterson AFB, OH 45433-7251
Tel: (937)255-6016/Fax: (937)255-3211

ABSTRACT

Conventional DC/DC converter topologies contain a single semiconductor switch, a diode, and various arrangements of inductors and capacitors to filter the resulting waveforms into low ripple DC. The output or input voltage is limited to the rating of the semiconductor switch and diode. For high voltge performance, transformers are added to form forward, flyback, or push-pull topologies. For high input voltages, semiconductor switches are arranged in an inverter bridge topology with a transformer to operate at higher voltages. Generally, conventional DC/DC converters are limited to low voltage applications. The addition of a transformer to provide sufficient voltage gain adds significant weight to the converter. Series, parallel resonant circuits with dual bridge circuits can function like a DC/DC converter with a transformer. Resonant converter topologies concepts have existed for the past 30 years. This paper will present a simplied generalized view of resonant circuits as π-filters and T-filters which give insight into improving circuit performance and developing new resonat topologies for bidirectional power flow.

INTRODUCTION

Switch-mode power converters generally have the disadvantage of producing losses when the converter attempts to abruptly turn off current while simultaneously attempting to standoff a voltage across the same switch. In reality, the current has a gradual decay with a rising voltage producing power that is not dissipated usefully in the load. Various types of resonant circuits give the power circuit the ability to turn off at a zero point in the resulting sinusoidal waveform, helping to reduce power losses. This reduction in losses permits high frequency operation of the switches, which in turn reduces the size of capacitors, inductors and transformers, making resonant converters relatively small even at high power levels.

Resonant circuits were applied to silicon controlled rectifiers (SCR) to make these early converter circuits efficient and smaller in size. Early SCR's would turn off relatively slow (20μs typically) so that any voltage present would produce power losses. SCR's could not tolerate large dV/dt and would actually turn on again if enough delay was given before full voltage appeared across the switch. Finally, early SCR's could not tolerate large dI/dt at turnon since the current carriers a limited to a small area, which looks like a high resistance and therefore high power dissipation. The power dissipation was usually high enough to cause hot spots that would burn the SCR out if dI/dt were too large. Resonant circuits produced zero current and voltage points to allow "soft" turnon and turnoff of the switch.

Traditionally, resonant converters are categorized into three types: series, parallel, and series-parallel. The series resonant converter contains a resonant circuit in series with the load and the parallel resonant converter contains a resonant circuit in parallel with the load. The series-parallel converter contains a resonant circuit parallel to the load with a series resonant circuit connected between the power source and parallel combination. The three conventional categories of resonant circuits can be viewed as subsets of π-filter and T-filter circuits. Using a simple impedance model gives a reasonable qualitative analysis of the influence of the different circuit elements on voltage and current. The simplified models gives a clearer picture if adding extra components will change the performance of the converter. Studies have shown that resonant π-filters and T-filters can act as voltage boost circuits or "resonant transformers." A high power resonant voltage step up converter for a MHD power conditioner was designed by Maxwell Laboratories in 1976 converting 30 KW, 2.5 KV source to 27 MW, 20 KV and a 3 MW, 200 KV.

Filter models easily apply to any type of resonant converter and with some stretch of the imagination, the analysis can apply to quasi-resonant circuits. A simplified analysis is basically

representing each inductive or capacitive element (or combination) as a simple impedance Z. The effects of initial voltage and current conditions are lost, however, important effects such a power quality, the degree of isolation of source and load, and bi-directional compatibility can be assessed.

VOLTAGE-FED π-FILTER TOPOLOGY

Fig. 1 shows a conceptual converter topology using a generalized π-filter fed by a constant voltage source with a Thevin equivalent source impedance.

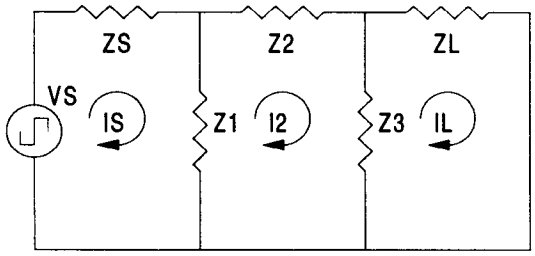

Fig. 1 - Voltage Fed π-filter converter

Switch-mode inverter generally have four basic states consisting of a positive on state, an off-state, a negative on state, and a final off-state. The dead-time state is usually required for to turn-off switches like thyristors and prevent shorting the power bus. In addition, the off-state helps to reduce dV/dt power losses.

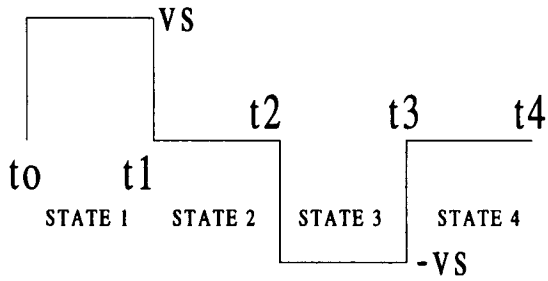

Fig. 2 - Switching States

The state equations are written in the frequency domain to produce simple algebraic relations. States 1 & 3 are basically equivalent circuits, where only polarity of the source changes. The simplified analysis ignores initial conditions which are require to determine the currents and voltages in States 2 & 4. Only a detailed analysis for specific circuit elements can fully account for the effects of initial voltage and current.

For the circuit shown in Fig. 1, the loop equations for State 1 (t0 < t < t1), VS(t) = VS, VS(s) = VS/s, (droping the conventional frequency notation "s"),

$$\frac{VS}{s} = ZS\cdot IS + Z1\cdot(IS - I2)$$

$$0 = Z1\cdot(I2 - IS) + Z2\cdot I2 + Z3\cdot(I2 - IL)$$

$$0 = Z3\cdot(IL - I2) + ZL\cdot IL \qquad (1)$$

The load current IL becomes,

$$IL = \frac{VS}{s\cdot ZL}\cdot\frac{1}{\left[\left(\frac{1}{ZL}+\frac{1}{Z3}\right)\cdot(Z2+Z1)+1\right]\cdot\frac{ZS}{Z1}+\left(\frac{1}{Z3}+\frac{1}{ZL}\right)\cdot Z2+1} \qquad (2)$$

We see that Z3 and ZL work in parallel and that the source impedance ZS and the series impedance Z2 have an influence on the performance of the circuit. A non-zero source impedance interacts with every impedance in the circuit. For minimal source impedance (ZS ≡ 0), the load current simplifies to,

$$IL = \frac{VS}{s\cdot ZL}\cdot\frac{1}{\left(\frac{1}{Z3}+\frac{1}{ZL}\right)\cdot Z2+1} \qquad (3)$$

The load voltage (VL = ZL IL) is given by,

$$VL = \frac{VS}{s}\cdot\frac{1}{\left[\left(\frac{1}{ZL}+\frac{1}{Z3}\right)\cdot(Z2+Z1)+1\right]\cdot\frac{ZS}{Z1}+\left(\frac{1}{Z3}+\frac{1}{ZL}\right)\cdot Z2+1} \qquad (4)$$

and again for minimal source impedance,

$$VL = \frac{VS}{s}\cdot\frac{1}{\left(\frac{1}{Z3}+\frac{1}{ZL}\right)\cdot Z2+1} \qquad (5)$$

The source current becomes,

$$IS = \frac{VS}{s\cdot Z1}\cdot\frac{\left(\frac{1}{ZL}+\frac{1}{Z3}\right)\cdot(Z2+Z1)+1}{\left[\left(\frac{1}{ZL}+\frac{1}{Z3}\right)\cdot(Z2+Z1)+1\right]\cdot\frac{ZS}{Z1}+\left(\frac{1}{Z3}+\frac{1}{ZL}\right)\cdot Z2+1} \qquad (6)$$

The source current is a major component of power quality seen by the power system and all of the component effect power quality. The source current for minimal source impedance is,

$$IS = \frac{VS}{s\cdot Z1}\cdot\frac{\left(\frac{1}{ZL}+\frac{1}{Z3}\right)\cdot(Z2+Z1)+1}{\left(\frac{1}{Z3}+\frac{1}{ZL}\right)\cdot Z2+1} \qquad (7)$$

The voltage gain from source to load is given by,

$$\frac{VL}{VS} = \frac{1}{\left[\left(\frac{1}{ZL}+\frac{1}{Z3}\right)\cdot(Z2+Z1)+1\right]\cdot\frac{ZS}{Z1}+\left(\frac{1}{Z3}+\frac{1}{ZL}\right)\cdot Z2+1} \qquad (8)$$

We see the π-filter circuit is a natural buck circuit. To produce a voltage boost, the initial capacitor voltage must be higher than the source voltage or a transformer must be added.

The voltage gain for minimal source impedance,

$$\frac{VL}{VS} = \frac{1}{\left(\frac{1}{Z3}+\frac{1}{ZL}\right)\cdot Z2+1} \tag{9}$$

When ZS << Z1, the influence of ZS can be minimized. If Z3 is open (Z3 = ∞) then the circuit simplifies to a classic series converter which is a really a narrow bandpass filter. For bi-directional power flow in a voltage-fed π-filter topology, given Z2 remains the same, the value of Z3 can be adjusted to produce a good impedance match with ZL. For State 2 and State 4, the solutions are IS(s) = 0 and IL(s) = 0 when the initial conditions are ignored. For State 3 the solutions for current and voltage are the negatives of State 1.

VOLTAGE-FED T-FILTER TOPOLOGY

Fig. 3 shows a conceptual converter using a generalized T-filter with a constant voltage source using a Thevin equivalent impedance

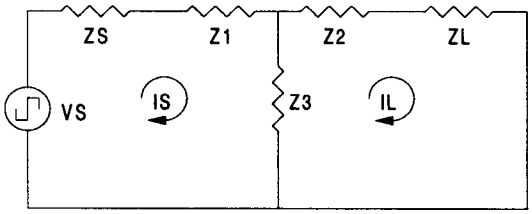

Fig. 3 - Voltage fed T-filter converter

The loop equations in State 1 where t0 < t < t1, VS(s) = VS/s, are,

$$\begin{aligned} \frac{VS}{s} &= ZS\cdot IS + Z1\cdot IS + Z3\cdot(IS-IL) \\ 0 &= Z3\cdot(IL-IS) + Z2\cdot IL + ZL\cdot IL \end{aligned} \tag{10}$$

The load current becomes,

$$IL = \frac{VS}{s\cdot ZL}\cdot\frac{1}{\left(1+\frac{Z2+ZL}{Z3}\right)\cdot\frac{ZS+Z1}{ZL}+\frac{Z2}{ZL}+1} \tag{11}$$

All circuit elements interact even if ZS is minimized (ZS = 0),

$$IL = \frac{VS}{s\cdot ZL}\cdot\frac{1}{\left(1+\frac{Z2+ZL}{Z3}\right)\cdot\frac{Z1}{ZL}+\frac{Z2}{ZL}+1} \tag{12}$$

The circuit will produce a more complex frequency response, which may be desired for some applications. Impedance matching would be difficult, making this topology less suited for bi-directional power flow.

The load voltage is again given by VL = ZL IL,

$$VL = \frac{VS}{s}\cdot\frac{1}{\left(1+\frac{Z2+ZL}{Z3}\right)\cdot\frac{Z1+ZS}{ZL}+\frac{Z2}{ZL}+1} \tag{13}$$

For the case of minimal source impedance,

$$VL = \frac{VS}{s}\cdot\frac{1}{\left(1+\frac{Z2+ZL}{Z3}\right)\cdot\frac{Z1}{ZL}+\frac{Z2}{ZL}+1} \tag{14}$$

The source current has a complex frequency response,

$$IS = \frac{VS}{s\cdot ZL}\cdot\frac{1+\frac{ZL+Z2}{Z3}}{\left(1+\frac{Z2+ZL}{Z3}\right)\cdot\frac{Z1+ZS}{ZL}+\frac{Z2}{ZL}+1} \tag{15}$$

and even for minimal source impedance,

$$IS = \frac{VS}{s\cdot ZL}\cdot\frac{1+\frac{ZL+Z2}{Z3}}{\left(1+\frac{Z2+ZL}{Z3}\right)\cdot\frac{Z1}{ZL}+\frac{Z2}{ZL}+1} \tag{16}$$

indicating more complications for power quality compared to the voltage fed π-filter converter. Finally the source to load voltage gain is,

$$\frac{VL}{VS} = \frac{1}{\left(1+\frac{Z2+ZL}{Z3}\right)\cdot\frac{Z1+ZS}{ZL}+\frac{Z2}{ZL}+1} \tag{17}$$

and for minimal source impedance,

$$\frac{VL}{VS} = \frac{1}{\left(1+\frac{Z2+ZL}{Z3}\right)\cdot\frac{Z1}{ZL}+\frac{Z2}{ZL}+1} \tag{18}$$

which implies a natural voltage step-down.

CURRENT-FED PI-FILTER TOPOLOGY

Fig. 4 shows a conceptual DC/DC converter using a generalized resonant π-filter and a constant current source represented with a Norton equivalent impedance.

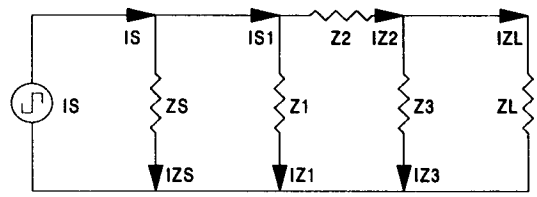

Fig 4 - Current-Fed π-filter converter

The nodal equations for the current fed π-filter converter shown in Fig 4 easily determine since there are only two node voltages, VS and VL. For State 1 (t0 < t < t1), IS(s) = IS/s,

$$\begin{aligned} \frac{IS}{s} &= \frac{VS}{Z1} + \frac{VS - VL}{Z2} + \frac{VS}{ZS} \\ 0 &= \frac{VL - VS}{Z2} + \frac{VL}{Z3} + \frac{VL}{ZL} \end{aligned} \tag{19}$$

The solution for load voltage is given by,

$$VL = \frac{ZL \cdot IS}{s} \cdot \frac{1}{\left[\left(\frac{1}{ZS} + \frac{1}{Z1}\right) \cdot (Z2 + Z3) + 1\right] \cdot \frac{ZL}{Z3} + \left(\frac{1}{Z1} + \frac{1}{ZS}\right) \cdot Z2 + 1} \tag{20}$$

If the source impedance is maximized (ZS ≅ ∞), the load voltage becomes,

$$VL = \frac{ZL \cdot IS}{s} \cdot \frac{1}{\left(\frac{Z2 + Z3}{Z1} + 1\right) \cdot \frac{ZL}{Z3} + \frac{Z2}{Z1} + 1} \tag{21}$$

The load current (IL = VL/ZL) is then,

$$IL = \frac{IS}{s} \cdot \frac{1}{\left[\left(\frac{1}{ZS} + \frac{1}{Z1}\right) \cdot (Z2 + Z3) + 1\right] \cdot \frac{ZL}{Z3} + \left(\frac{1}{Z1} + \frac{1}{ZS}\right) \cdot Z2 + 1} \tag{22}$$

Even for a large source impedance, the load current is

$$IL = \frac{IS}{s} \cdot \frac{1}{\left(\frac{Z2 + Z3}{Z1} + 1\right) \cdot \frac{ZL}{Z3} + \frac{Z2}{Z1} + 1} \tag{23}$$

The load current has a complicated frequency response making impedance matching difficult. The source voltage becomes,

$$VS = \frac{ZL \cdot IS}{s} \cdot \frac{\left(1 + \frac{Z2}{Z3}\right) + \frac{Z2}{ZL}}{\left[\left(\frac{1}{Z1} + \frac{1}{ZS}\right) \cdot (Z2 + Z3) + 1\right] \cdot \frac{ZL}{Z3} + \left(\frac{1}{Z1} + \frac{1}{ZS}\right) \cdot Z2 + 1} \tag{24}$$

so that power quality is more difficult to manage even for large source impedance,

$$VS = \frac{ZL \cdot IS}{s} \cdot \frac{1 + \frac{Z2}{Z3} + \frac{Z2}{ZL}}{\left(\frac{Z2 + Z3}{Z1} + 1\right) \cdot \frac{ZL}{Z3} + \frac{Z2}{Z1} + 1} \tag{25}$$

The source to load current gain is,

$$\frac{IL}{IS} = \frac{1}{\left[\left(\frac{1}{ZS} + \frac{1}{Z1}\right) \cdot (Z2 + Z3) + 1\right] \cdot \frac{ZL}{Z3} + \left(\frac{1}{Z1} + \frac{1}{ZS}\right) \cdot Z2 + 1} \tag{26}$$

for the large source impedance, the current gain becomes,

$$\frac{IL}{IS} = \frac{1}{\left(\frac{Z2 + Z3}{Z1} + 1\right) \cdot \frac{ZL}{Z3} + \frac{Z2}{Z1} + 1} \tag{27}$$

The current gain indicates the circuit has a natural tendency to reduce current.

CURRENT-FED T-FILTER TOPOLOGY

Finally, the conceptual converter using a T-filter and a constant current source represented with a Norton equivalent impedance is shown in Fig. 5.

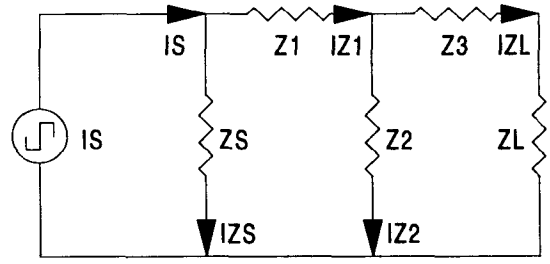

Fig. 5 - Current-Fed T-filter converter

The nodal equations for the current-fed T-filter converter for State 1 where t0 < t < t1, IS(t) = IS, IS(s) = IS/s,

$$\begin{aligned} \frac{IS}{s} &= \frac{VS}{ZS} + \frac{VS - V2}{Z1} \\ 0 &= \frac{V2 - VS}{Z1} + \frac{V2}{Z2} + \frac{V2 - VL}{Z3} \\ 0 &= \frac{VL - V2}{Z3} + \frac{VL}{ZL} \end{aligned} \tag{28}$$

The load voltage becomes,

$$VL = \frac{ZL \cdot IS}{s} \cdot \frac{1}{\left(\frac{Z1 + Z2}{ZS} + 1\right) \cdot \frac{ZL + Z3}{Z2} + \frac{Z1}{ZS} + 1} \tag{29}$$

which indicates that Z3 and ZL naturally work in series but that Z1 and Z2 work in series. If ZS >> Z1 + Z2 (large source impedance), the load voltage reduces to,

$$VL = \frac{ZL \cdot IS}{s} \cdot \frac{1}{\frac{ZL + Z3}{Z2} + 1} \tag{30}$$

If Z3 = 0, the current-fed T-filter topology simplifies to a classical parallel converter. In the bi-directional case where Z2 remains the same, Z3 can be chosen to match the converter impedance to the load impedance easily.

The load current is given by,

$$IL = \frac{IS}{s} \cdot \frac{1}{\left(\frac{Z1 + Z2}{ZS} + 1\right) \cdot \frac{ZL + Z3}{Z2} + \frac{Z1}{ZS} + 1} \tag{31}$$